

Road Surface Noise

Measurement of the Acoustic
Absorption of Porous Asphaltic Mix
Surfaces

Client: NZ Transport Agency - Waka Kotahi
Date: 29th May 2024
Ref: 23-117-R04-B



Prepared for (the Client)
NZ Transport Agency - Waka Kotahi

Prepared by the Consultant)
Altissimo Consulting Ltd

Project Road Surface Noise
Report Measurement of the Acoustic Absorption of Porous Asphaltic Mix Surfaces
Reference 23-117-R04-B

Prepared by

George Bell
Consultant

Reviewed by

Robin Wareing
Principal Acoustic Engineer

Version history:

Version	Date	Comment
A	09-052024	Release for client review.
B	29-05-2024	Updated with client feedback.

Report disclaimer and limitations:

This report has been prepared in accordance with the usual care and thoroughness of the consulting profession for the use of the Client. It is based on generally accepted practices and standards at the time it was prepared. No other warranty, expressed or implied, is made as to the professional advice included in this report.

This report should be read in full. No responsibility is accepted for use of any part of this report in any other context or for any other purpose or by third parties. This report does not purport to give legal advice. Legal advice can only be given by qualified legal practitioners.

Document Copyright © Altissimo Consulting Ltd

Abstract

This report presents the results from the measurement of the acoustic absorption of porous asphaltic mix surfaces. The aims of this investigation were to determine the efficacy of the methodology and explore the changes in acoustic absorption with surface properties such as thickness and void fraction.

The study utilised the in situ extended surface method described in ISO 13472-1 to measure the acoustic absorption of 109 discrete points across four surface types on the Christchurch Northern Corridor.

The test apparatus successfully measured the absorption of porous asphaltic mixes. Analyses of the measured data demonstrated alignment with the expected theoretical behaviours. Two measurement issues were identified, which include the presence of anomalous peaks across all measurements and an unexpected sound being emitted from the speaker.

Increasing thickness was observed to cause a reduction in the frequency of the absorption peaks. The comparison of the absorption of epoxy-modified and standard porous asphalt was inconclusive. There were insufficient data to demonstrate the influence of void fraction on absorption.

It is recommended that further measurements are undertaken with the system to expand the understanding of the interaction between acoustic absorption and tyre/road noise.

Contents

Abstract	ii
Glossary.....	iv
1 Introduction	1
2 Sound Absorption Measurement	2
2.1 ISO 13472-1	2
2.2 Hardware and Data Acquisition	3
2.3 Measurements.....	3
2.4 Reflective Surface	4
3 Other Data	5
4 Results	6
4.1 Sample of EPA7 (50 mm)	7
4.2 All EPA7 (50 mm).....	8
4.3 EPA7 Thickness	9
4.4 EPA versus PA	11
4.5 Preliminary Void Fraction Comparison	13
5 Future Research.....	14
5.1 Method	14
5.2 Measurements.....	14
5.3 Analyses.....	14
6 Conclusions	15
References	16
Appendix A - Additional Data	17
Appendix B - Theoretical Absorption	18
Appendix C - Lane Labelling	21

Glossary

α_0	Sound absorption coefficient at normal incidence
CNC	Christchurch Northern Corridor
CPX	Close proximity
CSM2	Christchurch Southern Motorway - Stage 2
EPA	Epoxy-modified porous asphalt
Lane 2	Second-closest lane to the centre of the road (see Figure 14).
L_{CPX}	Close proximity sound pressure level
MLS	Maximum-length sequences
NB	Northbound
NDM	Nuclear densometer
NMAS	Nominal maximum aggregate size
PA	Porous asphalt
PA7 HS	Porous asphalt high strength
RS	Reference station
S2G	SH1 Johns Road from The Groynes to Sawyers Arms Road
SB	Southbound
SD	Standard deviation
SE	Standard error
SMA	Stone mastic asphalt
WBB	Western Belfast Bypass

1 Introduction

This study is a continuation of research into tyre/road noise led by Waka Kotahi (Noise and Vibration Research | Waka Kotahi NZ Transport Agency). The aim of this work was to determine the efficacy of the in-situ measurement of acoustic absorption of porous asphaltic mix surfaces.

Acoustic absorption (hereafter absorption) is known to have a significant impact on tyre/road noise. Theory suggests that porous asphaltic mix surfaces have frequency-dependent absorption characteristics that are a function of layer thickness, interconnected void fraction, air flow resistance, and void shape (Berengier et al., 1990). Descriptions of the theoretical influence of surface properties on absorption are included in Appendix B.

Absorption influences tyre/road noise received at the wayside by at least two mechanisms; (1) near-field absorption, particularly in the leading and trailing wedges between the tyre and the road surface (the “horn” effect) (Schutte et al., 2015), and (2) free-field absorption as sound propagates over the road surface to observers at the road side (Hamet, 2004).

ISO 13472-1 defines an in-situ method for the measurement of absorption. This method was utilised in this investigation to measure the absorption of several porous asphaltic mixes on the Christchurch Northern Corridor (CNC).

The objectives of this investigation were to:

- Measure the in situ acoustic absorption of porous asphaltic mix surfaces using the extended surface method described in ISO 13472-1.
- Confirm the efficacy of the measurement method.
- Determine how absorption changes with physical surface properties (e.g., thickness and void fraction).

This report includes a description of the methodology followed by the results. The report concludes with a series of recommendations of potential system improvements, measurements, and analyses.

Exploration of the relationships between absorption and tyre/road noise, and the validation of a theoretical porous absorption model are not included in this report.

2 Sound Absorption Measurement

2.1 ISO 13472-1

The measurement of absorption followed ISO 13472-1:2022 (full title: Acoustics – Measurement of sound absorption properties of road surfaces in situ – Part 1: Extended surface method). A brief description of the method and details of specific parameters used within this investigation are included in this section.

The setup, shown schematically in Figure 1, comprises a sound source, and a microphone. The speaker emits a wave that travels to and reflects off the test surface. The microphone detects both the direct sound wave traveling towards the surface and the wave reflected back from the surface.

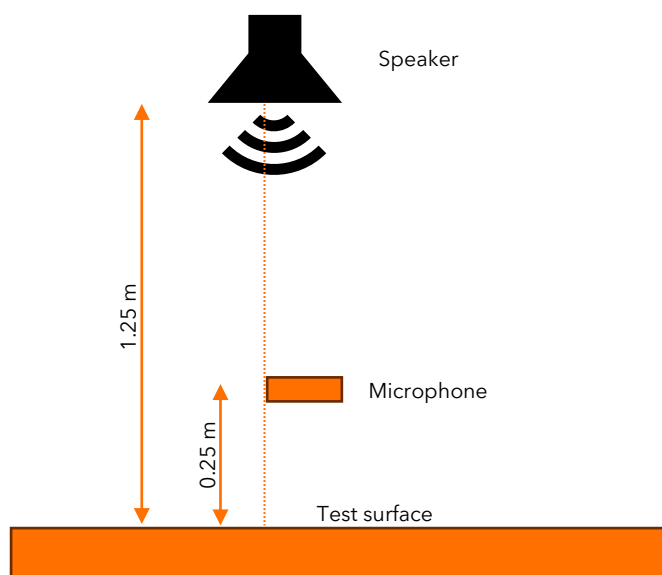


Figure 1: Diagram of the speaker, microphone, and test surface.

The method involves isolating the reflected component from the overall impulse response using a signal subtraction technique. The total impulse response is captured with the configuration in Figure 1 and contains both direct and reflected components. The direct component is identified through a free-field measurement, where the speaker and microphone are orientated upwards (i.e., the microphone is 1 m above the speaker). The direct component is subtracted from the total impulse response. This subtraction removes the direct sound pathway, leaving only the reflected component. The reflected component is then used to calculate the acoustic absorption.

The applicable frequency range is from 250 to 4,000 Hz. The measured area is within a radius of 1.34 m from the axis of the microphone and speaker. The speaker and microphone are 1.25 and 0.25 ± 0.01 m above the surface, respectively.

2.2 Hardware and Data Acquisition

The data acquisition system consisted of the following components:

- National Instruments cDAQ chassis with analogue output and microphone input cards
- 900 W amplifier
- 10" speaker
- ½" microphone

A nominal sample rate of 51.2 kHz was used for both the input and output signals.

A 16-bit maximum-length sequence (MLS) excitation signal was used for the impulse response measurement. Each cycle had a length of 65,535 samples (1.28 s long at 51.2 kHz sample rate). 30 repeated cycles were run for each measurement, giving a total duration of 38.4 s.

2.3 Measurements

All field measurements were undertaken during the night of 23-04-2024. The road surface was dry, and the air temperature varied from 10 to 13 °C. Measurements were taken with the speaker centred in the left (slow) lane of the southbound carriageway of CNC. The surfaces and measurement quantities are given in Table 1. The chainage of each measurement by surface type are given in Table 4 in Appendix A.

Table 1: Sample quantities by surface type.

Surface Type	Samples
EPA7 (30 mm)	23
EPA7 (50 mm)	44
PA7 (30 mm)	36
SMA10 (40 mm)*	6
Total	109

*SMA10 (40 mm) surfaces were on bridge decks.

The standard requires a minimum signal to noise ratio of 10 dB across all bands; the signal to noise ratio was above 30 dB for all bands for all measurement points. Free-field measurements were taken at the beginning and after every tenth measurement.

During the measurements, an unexpected anomalous buzzing noise was emanating from the speaker. The cause of this is currently unknown. It is expected that this did not significantly affect the results as the noise was present for both the free-field and downward measurements. Further investigation is required to identify and resolve the underlying issue.

The frequency alignment of the absorption curves has not been validated. It is recommended that this is undertaken prior to any further field measurements.

2.4 Reflective Surface

A painted concrete floor was measured as it theoretically approaches an acoustically fully reflective surface. The absorption curve for the painted concrete is shown in Figure 2. For comparison, the mean absorption for the six SMA10 (40 mm) measurements is also included. The frequencies of the peaks were consistently aligned between the concrete and SMA. The wavelengths of the peaks are approximately fractions of the 250 mm distance between the microphone and surface under test. There is no expectation that concrete and SMA would exhibit aligned absorption peaks; it is hypothesised that these peaks are an artefact of the measurement system. In addition, the reoccurring presence of negative absorption is not expected.

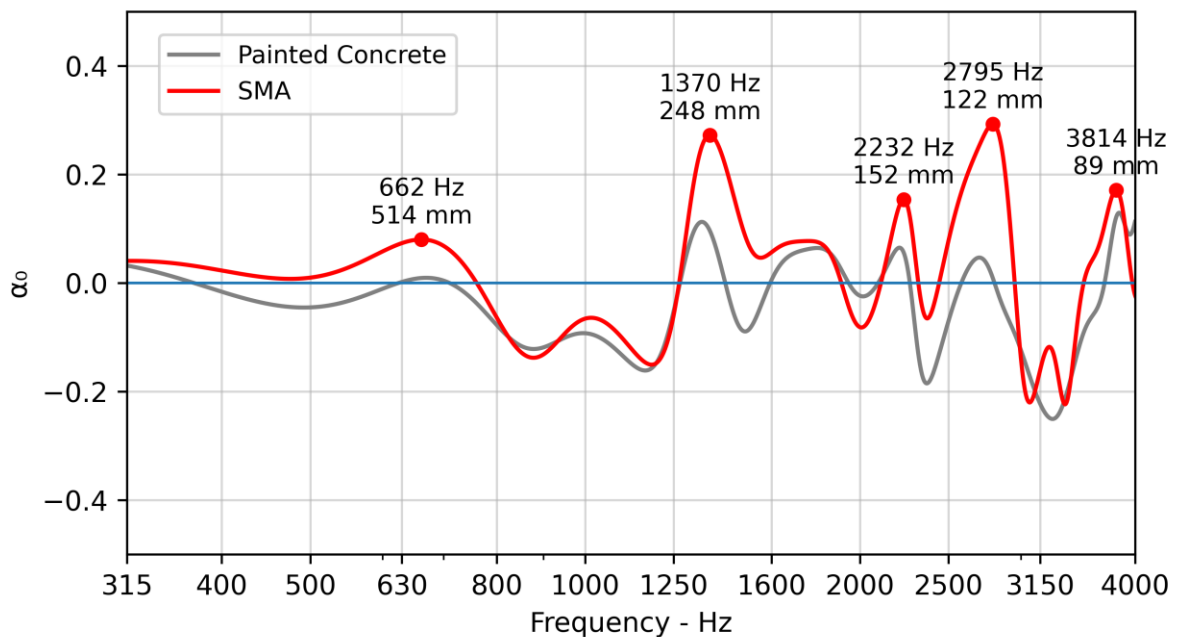


Figure 2: Absorption curves for painted concrete and SMA10 (40 mm) showing the frequency and wavelengths of peaks.

The appearance of these peaks represents a limitation of the measurement system and the collected data. In particular, the peak in the 1,300 to 1,400 Hz range overlaps with the first absorption peak of 30 mm thick surfaces, meaning the absorption in this range is unable to be confidently discerned.

The measurements still provide insightful data that can be used to understand the absorption characteristics of the assessed surfaces. Absorption values for frequencies below 1,200 Hz appear to be mostly unaffected by this artefact. The influence on absorption values above 1,200 Hz can be lessened by subtracting the measured absorption of painted concrete, which allows for tentative analyses using data in this range.

It is recommended that this is explored further and resolved prior to any future measurements.

3 Other Data

Details of other data sets referenced in the results are given in Table 2. Where thickness has been paired with an absorption measurement, the mean thickness was calculated for a circle with a 1 m radius around the axis of the speaker and microphone. Setting the radius to 1 meter was an arbitrary selection due to the uncertainty surrounding the precise radius of influence.

Table 2: Thickness and void fraction measurement details.

Data	Source	Longitudinal Resolution	Measurement Date
Thickness	Woods Mobile Survey	0.1 m	15-08-2021*
			07-06-2022*
Void fraction	Road Science	Discrete**	28-11-2023
			20-02-2024
			21-02-2024

*Dates are for the pre- and post-surfacing surveys; surfacing was undertaken in Feb and Mar 2022.

**The void fraction was measured at discrete points in the left wheel path and typically coincided with the absorption measurement locations.

4 Results

The following results are presented in this section:

- A single example of an absorption curve for one measurement of EPA7 (50 mm).
- Overlaid absorption curves for all EPA7 (50 mm) measurements.
- Mean absorption curves for EPA7 for thicknesses of 30, 40, and 50 ±3 mm.
- Frequency of first absorption peak as a function of thickness for EPA7.
- Mean absorption curves for EPA7 and PA7 with thicknesses of 30 ±3 mm.
- A preliminary point-to-point comparison of the effect of void fraction.

All results are the delta between the measured absorption and that of the painted concrete (Figure 2). This approach was taken to minimise the influence of peaks at wavelengths that are multiples of the distance between the microphone and the surface under test (see section 2.4). The peaks were present for all measured surfaces (i.e., painted concrete, SMA, and PA) but varied in amplitude. This represents a limitation of this investigation.

4.1 Sample of EPA7 (50 mm)

An example of the measured absorption curve for a single measurement point on the EPA7 (50 mm) surface is shown in Figure 3. The spectrum has distinct peaks in the measured range. The peak at 1,423 Hz is expected to be related to the measurement system artefact described above. The first and highest absorption peak occurred at 755 Hz. The peaks at 2,267 and 3,558 Hz are multiples of 3.0 and 4.7 of the first peak at 755 Hz. Theory suggests that the subsequent peaks occur at multiples of three and five times the first peak. The theoretical model presented by Berengier et al. (1990) (see Appendix B) was fitted to the measured data by aligning the frequency of the absorption peaks using the shape factor parameter. The absorption curve from the fitted model is included in Figure 3; there is good agreement between the measured and fitted absorption.

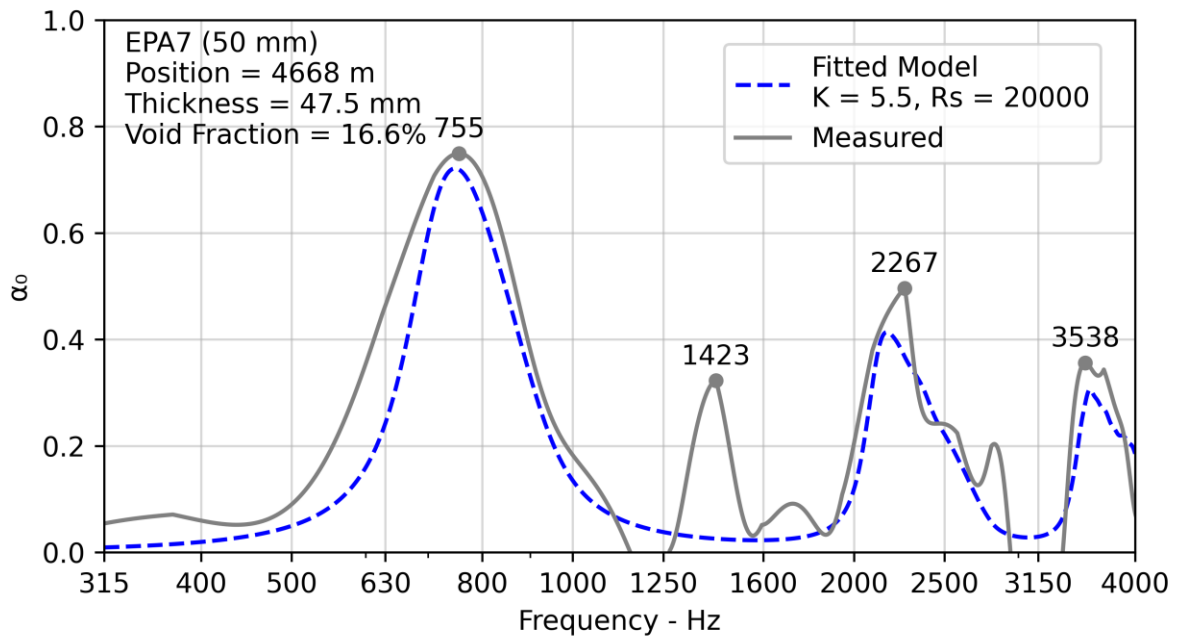


Figure 3: Absorption curve for a single measurement of EPA7 (50 mm).

4.2 All EPA7 (50 mm)

All absorption curves for the EPA7 (50 mm) surface are shown in Figure 4. There is significant variation in the curves, which is expected from the ranges of thickness and void fraction.

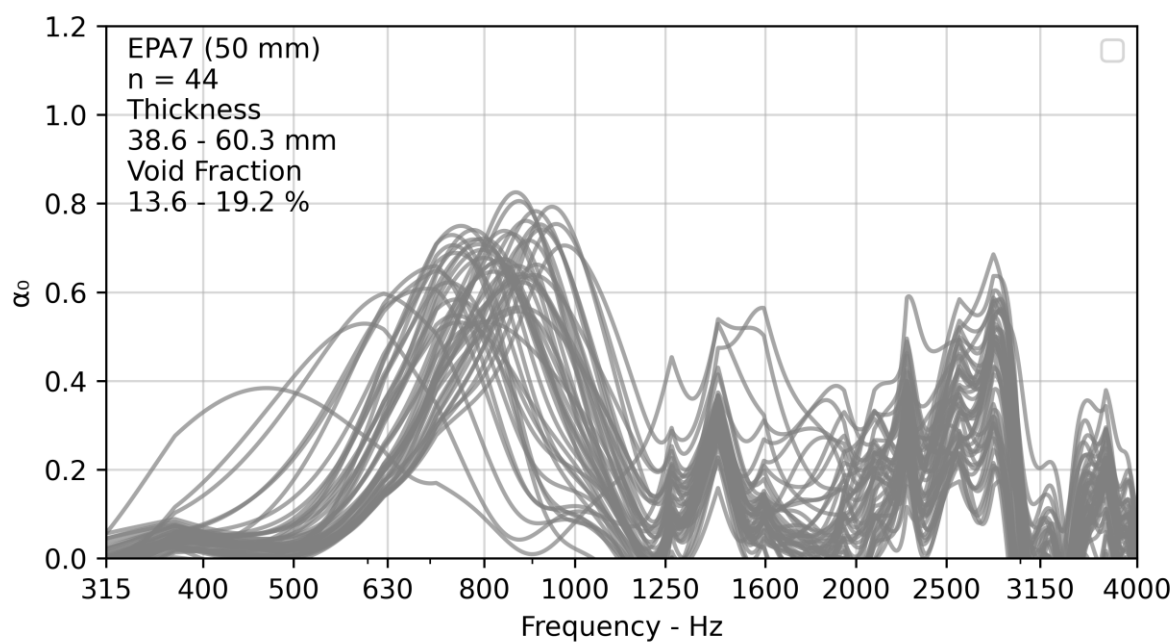


Figure 4: All absorption curves for EPA7 (50 mm).

4.3 EPA7 Thickness

The mean absorption curves for EPA7 grouped by thicknesses of 30, 40, and 50 \pm 3 mm are shown in Figure 5. The frequency of the first absorption peak was observed to decrease with increasing thickness.

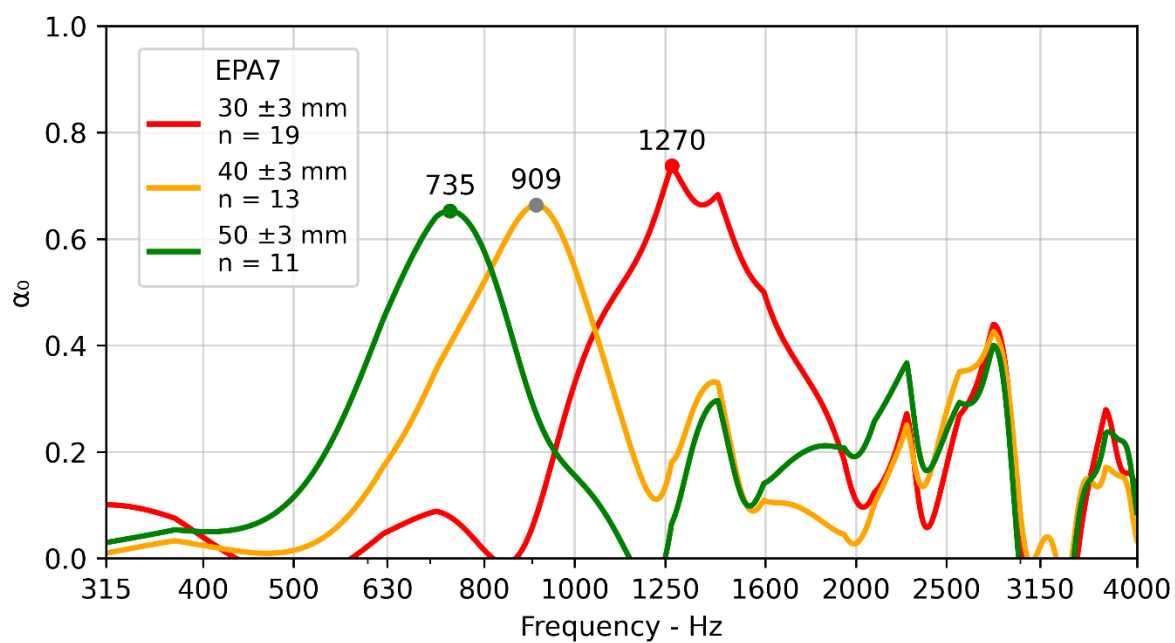


Figure 5: Mean absorption curves for EPA7 grouped by thickness.

The frequency of the first absorption peak is shown as a function of thickness in Figure 6. The frequency of the first absorption peak was negatively correlated with thickness. A second-order polynomial (Equation 1) was fitted to the measured data. The coefficients of the fitted model are given in Table 3. The fitted polynomial was a strong predictor of the frequency of the first absorption peak with an R^2 of 0.93 with the measured data.

The frequency of the first absorption peak predicted by the theoretical model described by Berengier et al. (1990) (see Appendix B) is included in Figure 6. A constant shape factor of 5.5 was used. The theoretical model predicts that the frequency of the first absorption peak will decrease with increasing thickness; this was observed in the measured data.

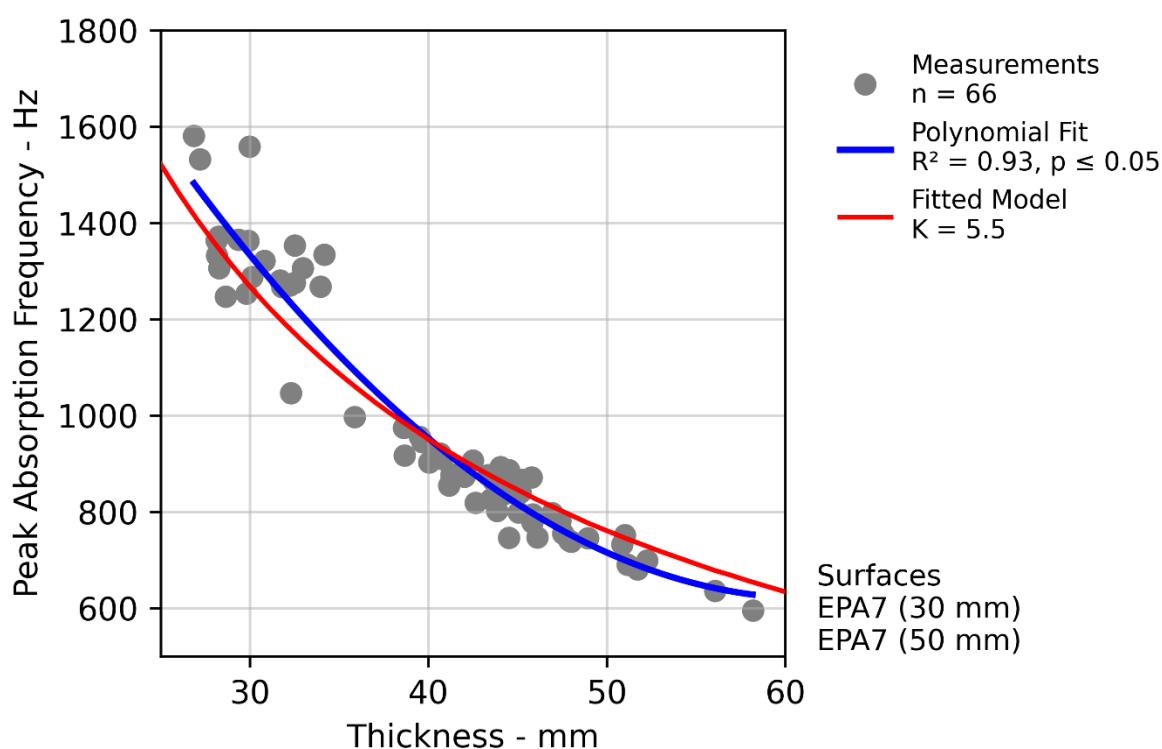


Figure 6: Frequency of the first absorption peak versus thickness for EPA7.

$$y = Ax^2 + Bx + C$$

Equation 1

Table 3: Coefficients of the fitted model between first peak absorption frequency and thickness.

Coefficient	Value	SE	P-Value
A	0.716	0.131	≤ 0.05
B	-88.2	10.6	≤ 0.05
C	3,335	206	≤ 0.05

4.4 EPA versus PA

The mean absorption curves for samples of EPA7 and PA7 with thicknesses of 30 ± 3 mm are given in Figure 7. The mean differences and standard deviations are given in Figure 8. At each frequency, a t-test was performed to determine if the mean difference was statistically significant ($p \leq 0.05$). The mean absorption for the EPA7 was observed to be 0.03 to 0.11 greater than that of the PA7 between 1,708 and 2,665 Hz. While a significant difference was observed at low frequencies (< 800 Hz), it is not expected to be physically meaningful due to the low absolute absorption values in this range (< 0.12). The frequencies of the peak absorption for both surfaces overlapped with one of the anomalous peaks at 1,370 Hz (see Section 2.4), which may have masked relevant information. There is insufficient evidence to indicate whether a significant difference in absorption exists between the EPA7 and PA7 (30 mm) surfaces on CNC. It is recommended to repeat the measurements and analysis after the measurement issues have been resolved.

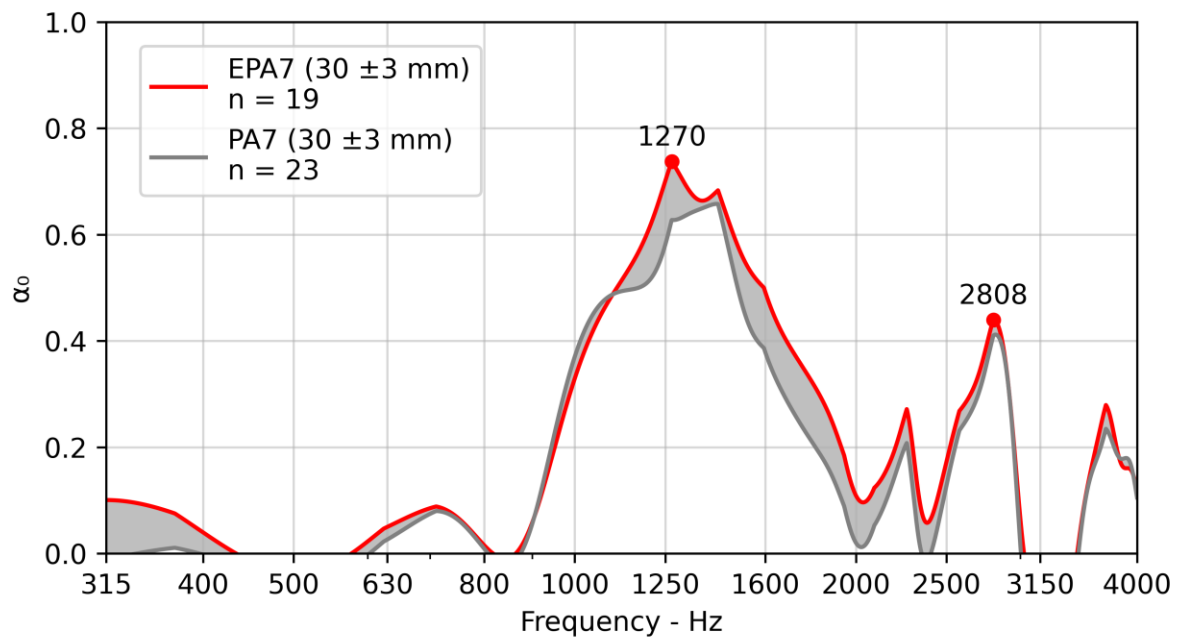


Figure 7: Mean absorption for EPA7 and PA7 (30 ± 3 mm).

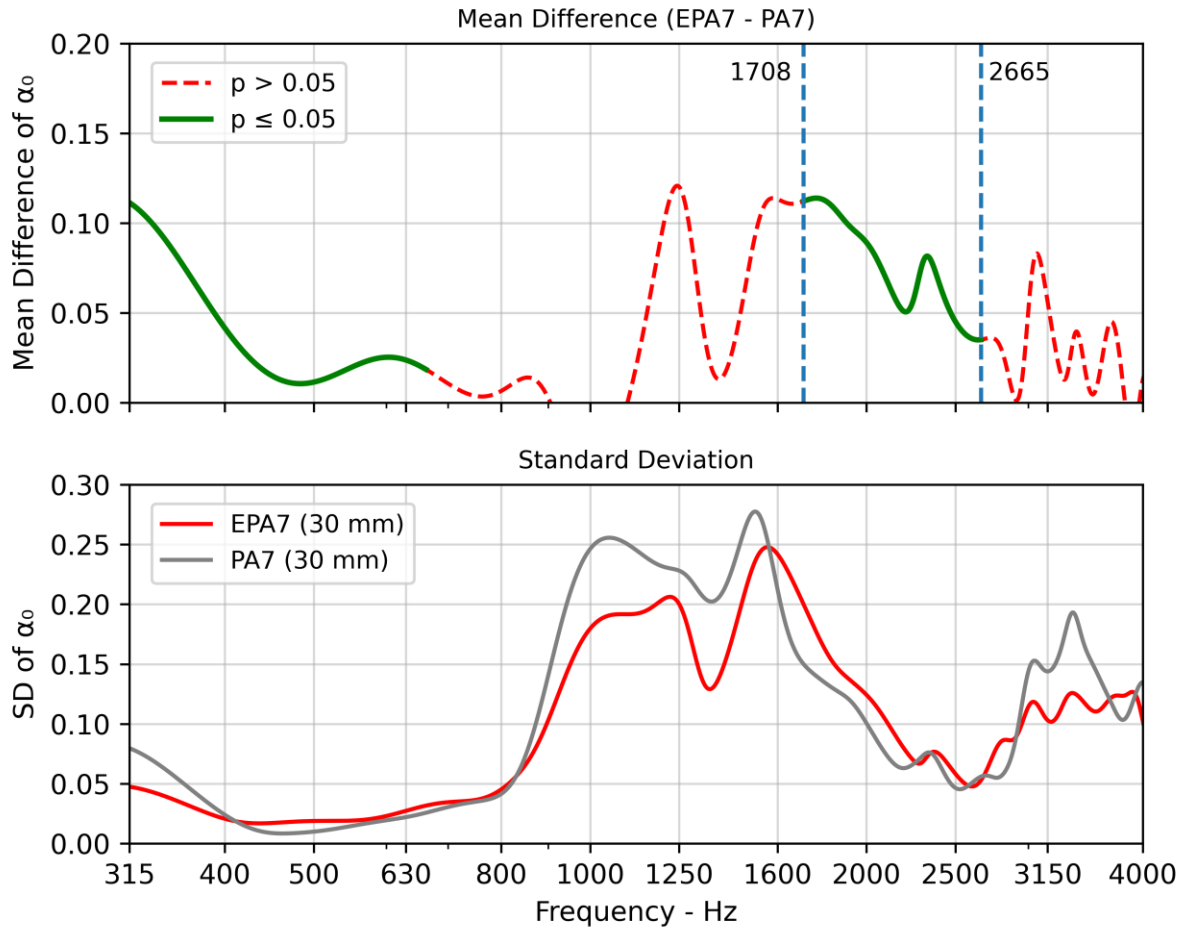


Figure 8: Mean differences and standard deviations of EPA7 and PA7 (30 mm) surfaces.

4.5 Preliminary Void Fraction Comparison

The void fraction range was insufficient to produce a detailed evaluation, however a preliminary comparison of two measurement points is given in Figure 9. The two points had equal mean thicknesses but different void fractions of 13.6 and 19.2% respectively. Between the two points, the one with the lower void fraction had a reduced frequency and amplitude of the first absorption peak. It is not known whether any or all differences in the absorption curves are attributable to void fraction.

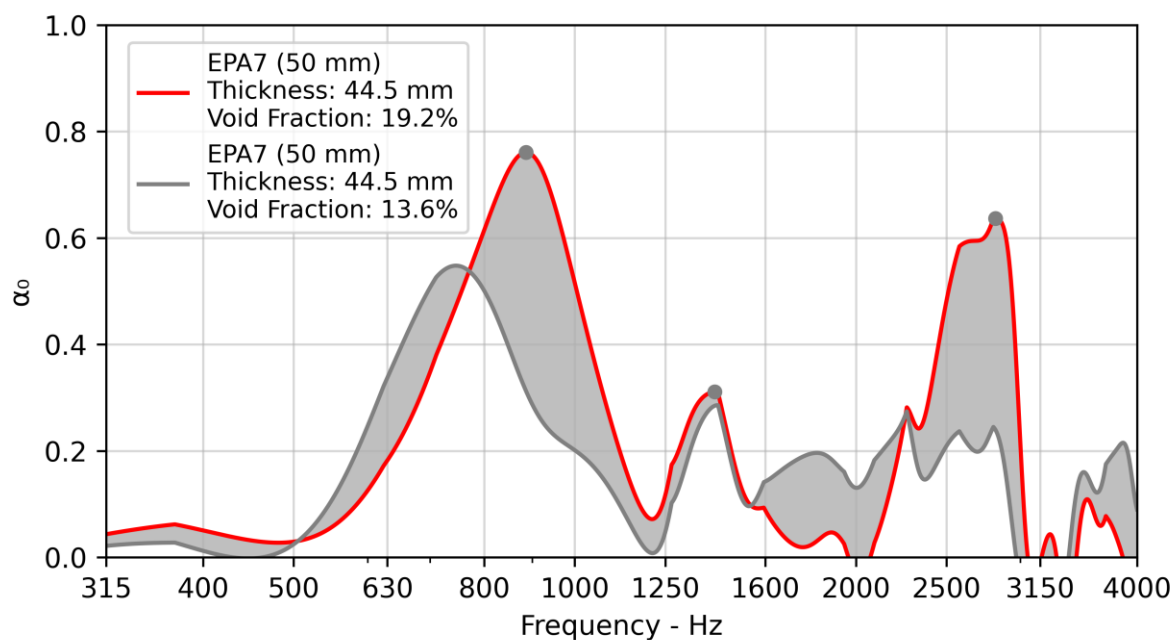


Figure 9: Absorption curves for two points of EPA7 (50 mm) with different void fractions.

5 Future Research

The following recommendations for future work are proposed grouped by method improvements, additional measurements, and potential analyses. It is recommended that the method issues are first addressed before further measurements are made on CNC; this will enable analyses of the relationships between tyre/road noise and absorption. The analyses will guide the prioritisation of any future measurements.

5.1 Method

- **Unexplained Absorption Peaks**
Identify the cause of absorption peaks that were present in all measurements and resolve the underlying issue.
- **Anomalous Speaker Noise**
Identify the cause of the anomalous speaker noise and resolve the underlying issue.
- **Frequency Alignment**
Verify the frequency alignment of the absorption curves.

5.2 Measurements

- **Thickness**
Capture further measurements on CNC to expand the relationship between thickness and absorption. In addition, measure WBB thickness trial sites and CSM2.
- **PA and EPA**
Remeasure the PA and EPA surfaces on CNC.
- **Void Fraction**
Measure additional trial sites (HS and LV) on CNC to expand the void fraction range. Concurrently measure void fraction (density) using the NDM (if not already captured).
- **Aggregate Size**
Measure surfaces with 10 mm NMAS such as the PA10 (30 mm) on CNC and the EPA10 (30 mm) mixes on S2G.
- **Site-to-Site**
Measure sites with the same nominal surface specifications (e.g., CSM2 and WBB).
- **Aged Surfaces**
Measure old surfaces (> 10 years) to provide an indication of change in absorption over time.

5.3 Analyses

- **Tyre/Road Noise**
Investigate the influence of absorption on L_{CPX} .
- **Theoretical Model**
Fit the measured data to a theoretical model and estimate other parameters such as shape factor and air flow resistance. Determine the variation of these fitted parameters.

6 Conclusions

The acoustic absorption of porous asphaltic mixes on CNC was measured in situ following ISO 13472-1. The test apparatus comprised of a vehicle-mounted speaker and microphone. 109 discrete points were measured across EPA7 (30 mm), EPA7 (50 mm), PA7 (30 mm), and SMA10 (40 mm) surfaces.

The resulting absorption curves closely resembled the expected form for porous absorbers, having discrete peaks and troughs. The frequency of the first absorption peak was observed to decrease with increasing thickness. The comparison of absorption for EPA7 and PA7 (30 mm) surfaces was inconclusive due to the overlap of the peak absorption frequencies and one of the anomalous peaks that persisted across all measurements. There were insufficient data to determine the influence of void fraction.

The test apparatus successfully measured the absorption of porous asphaltic mixes. Analyses of the measured data demonstrated alignment with the expected theoretical behaviours. The cause of the anomalous peaks that persisted across all measurements must be identified and resolved.

It is recommended that further measurements are undertaken with the system to expand the understanding of the interaction between acoustic absorption and tyre/road noise.

References

- Berengier, M., Hamet, J. F., & Bar, P. (1990). Acoustical Properties of Porous Asphalts: Theoretical and Environmental Aspects. *Transportation Research Record*, 1265. <https://trid.trb.org/view/348600>
- Hamet, J. F. (2004). *Reduction of tire road noise by acoustic absorption: Numerical evaluation of the pass-by noise level reduction using the normal incidence acoustic absorption coefficient*. 25p. <https://hal.science/hal-00546107>
- Noise and vibration research | Waka Kotahi NZ Transport Agency. (n.d.). Retrieved January 25, 2024, from <https://www.nzta.govt.nz/roads-and-rail/highways-information-portal/technical-disciplines/environment-and-sustainability-in-our-operations/environmental-technical-areas/noise-and-vibration/noise-and-vibration-research/#road-surface-noise-research>
- Schutte, J. H., Wijnant, Y. H., & de Boer, A. (2015). The Influence of the Horn Effect in Tyre/Road Noise. *Acta Acustica United with Acustica*, 101(4), 690–700. <https://doi.org/10.3813/AAA.918865>

Appendix A - Additional Data

Table 4: Measurement positions by surface type. All measurements are in the left lane of the southbound carriageway on CNC.

Surface Type	Measurement Locations Chainage - m
EPA7 (30 mm)	235.0, 257.0, 277.0, 299.2, 319.4, 339.1, 359.1, 379.1, 399.1, 419.3, 439.4, 459.4, 479.4, 499.4, 519.4, 539.6, 559.5, 579.5, 599.7, 619.4, 639.8, 659.3, 679.6, 700.4, 719.6, 739.7, 759.5, 778.3, 835.0, 854.8, 874.9, 894.8, 915.0
EPA7 (50 mm)	160.3, 179.4, 214.0, 235.0, 257.0, 277.0, 299.2, 319.4, 339.1, 359.1, 379.1, 399.1, 419.3, 439.4, 459.4, 479.4, 499.4, 519.4, 539.6, 559.5, 579.5, 599.7, 619.4, 639.8, 659.3, 679.6, 700.4, 719.6, 739.7, 759.5, 778.3, 835.0, 854.8, 874.9, 894.8, 915.0
PA7 (30 mm)	2368.1, 2388.2, 2408.2, 2428.4, 2448.5, 2468.3, 2488.3, 2508.4, 2528.6, 2547.9, 2568.5, 2588.0, 2608.8, 2628.6, 2648.5, 2668.2, 2688.2, 2708.4, 3127.8, 3137.7, 3147.3, 3157.8, 3167.8, 3177.3, 3187.2, 3197.4, 3207.6, 3217.5, 3227.7, 3237.6, 3247.7, 3257.2, 3267.0, 3277.3, 3287.4, 3297.4
SMA10 (40 mm)	795.0, 804.8, 1096.3, 1113.8, 4474.7, 4485.7

Appendix B - Theoretical Absorption

A theoretical model for the absorption curves of a porous surface was presented by Berengier et al. (1990). The key input parameters and their independent theoretical influence on absorption are presented in this appendix.

The model has input parameters of

- **Thickness (t):** The thickness of the porous layer in millimetres.
- **Void fraction (VF):** The interconnected volumetric fraction of free air in the voids of the porous layer.
- **Shape factor (K):** A dimensionless quantity that accounts for the non-linear paths within the voids.
- **Air flow resistance (Rs):** Specific air flow resistance in Rayls per centimetre.

The theoretical influences of each parameter on the absorption curve are presented below in Figure 10 to Figure 13. In each figure, one parameter is varied while holding the others constant.

The theoretical influences of each parameter are:

- **Thickness:** The peak absorption frequencies decrease with increasing thickness.
- **Void fraction:** The width of the absorption peaks increase with increasing void fraction. The absorption between peaks increases with increasing void fraction.
- **Shape factor:** The peak absorption frequencies decrease with increasing shape factor.
- **Air flow resistance:** The width of the absorption peaks increases with increasing air flow resistance. The peak absorption amplitude increases with increasing air flow resistance.

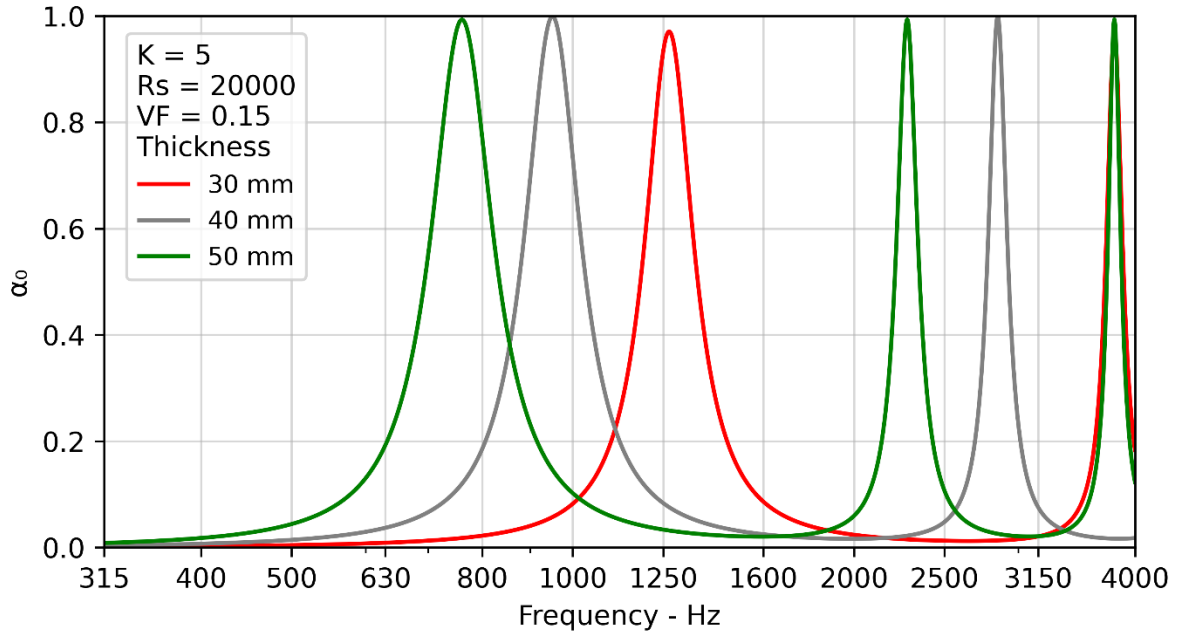


Figure 10: Theoretical influence of thickness on absorption.

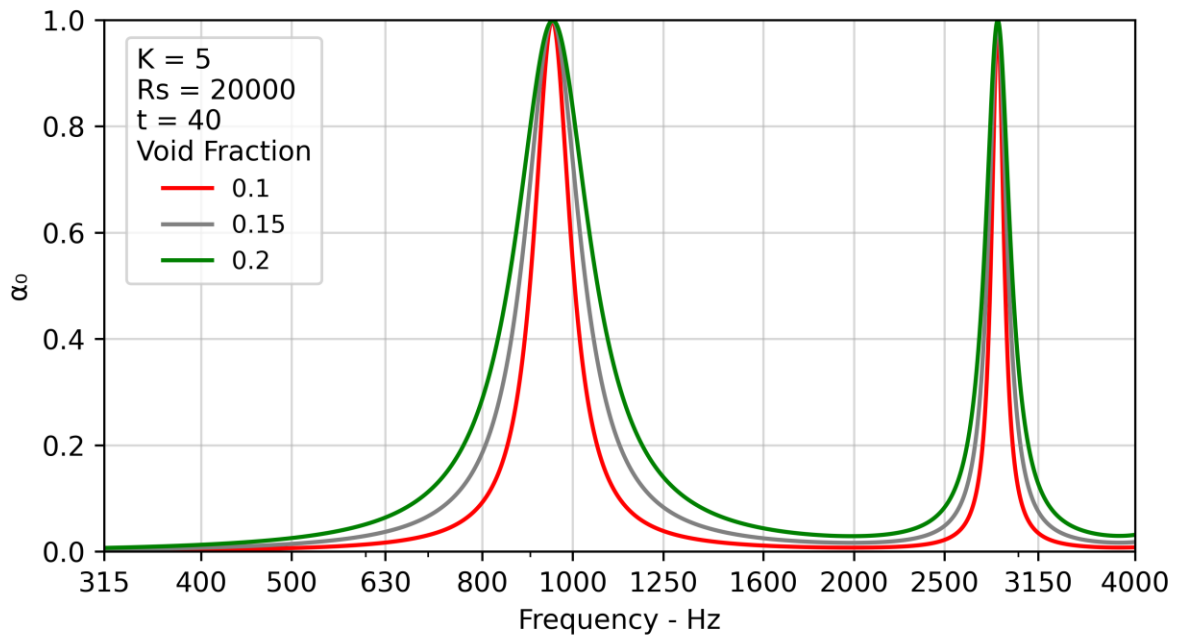


Figure 11: Theoretical influence of void fraction on absorption.

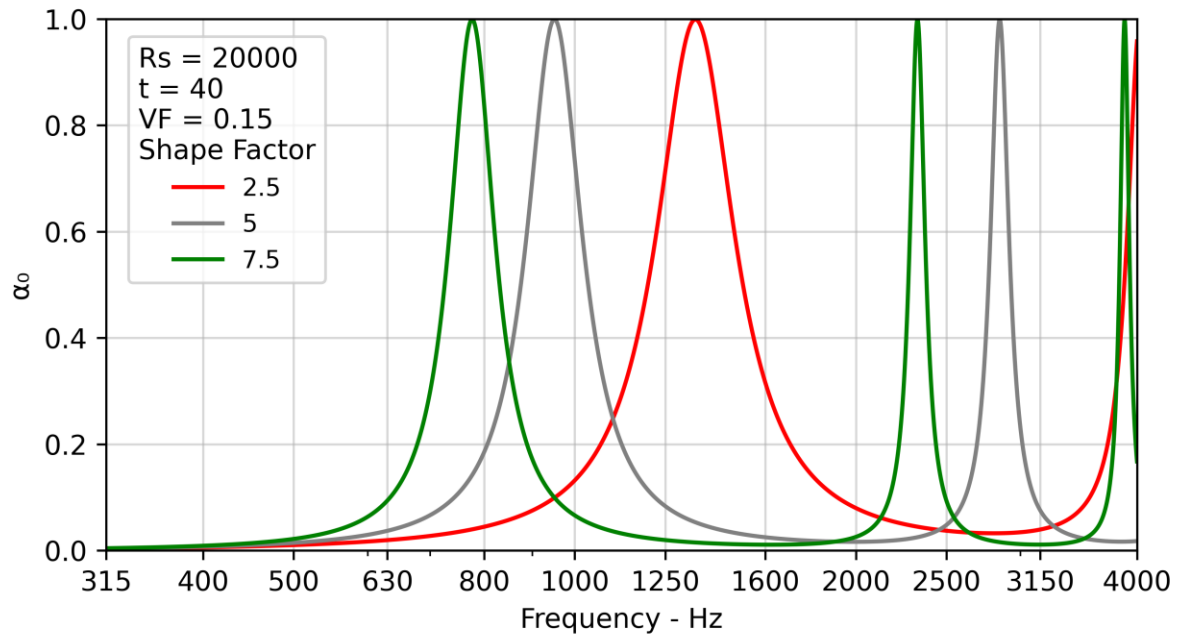


Figure 12: Theoretical influence of shape factor on absorption.

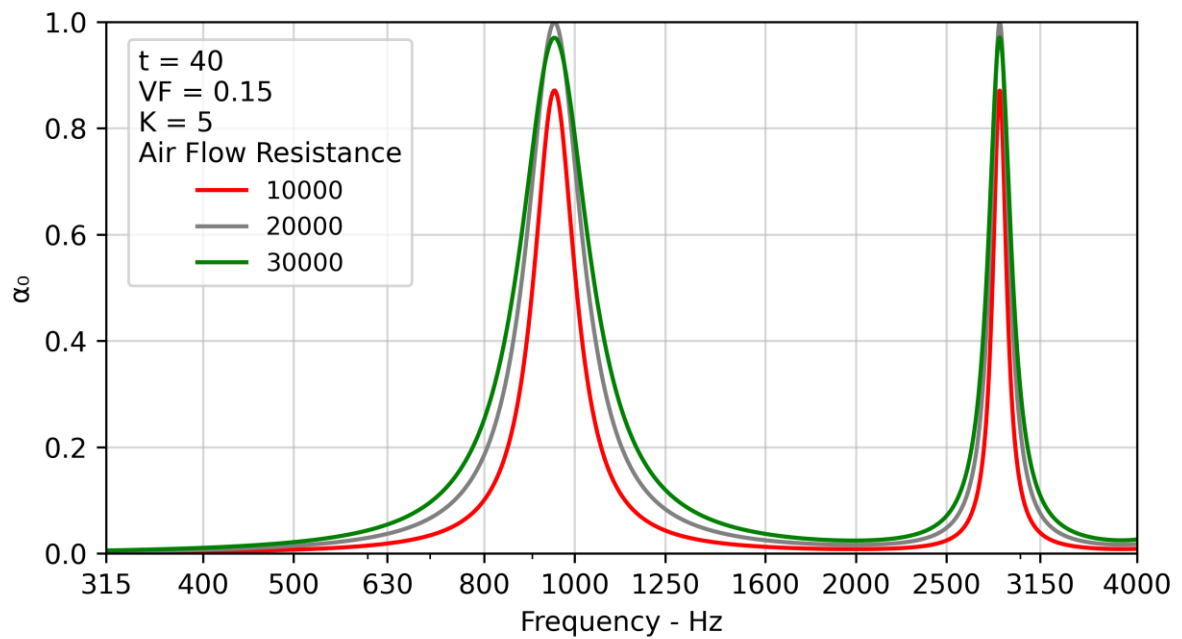
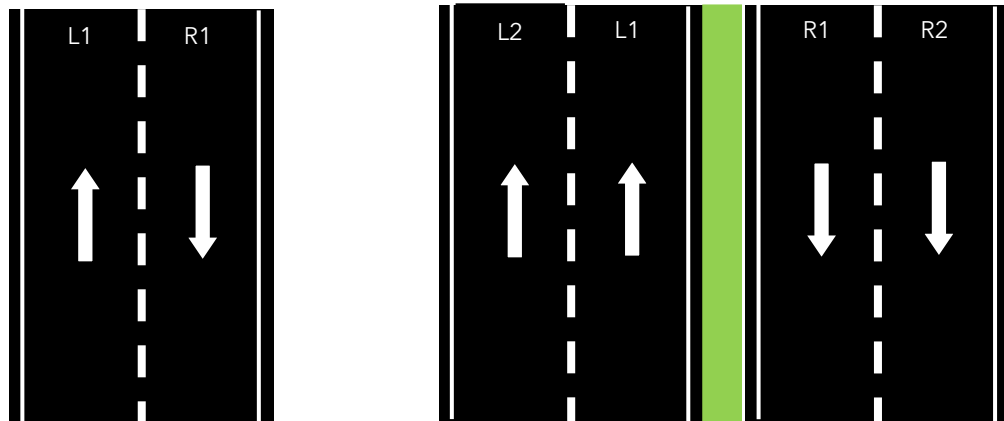


Figure 13: Theoretical influence of air flow resistance on absorption.

Appendix C - Lane Labelling



(a) Single carriageway

(b) Dual carriageway

Figure 14. Lane labelling convention (assuming increasing direction toward the top of the page).